

# Generative Adversarial Networks for Localized Vibrotactile Feedback in Haptic Surfaces

Camilo Hernandez-Mejia, Xiaotao Ren, Adrien Thabuis, Jonathan Chavanne, Paolo Germano, and Yves Perriard

*Laboratory of Integrated Actuators (LAI), École Polytechnique Fédérale de Lausanne (EPFL), Lausanne, Switzerland*

camilo.hernandez@epfl.ch (<name>.<last-name>@epfl.ch)

**Abstract**—Touch-screens are the most relevant interface in the context of human-computer interaction. Moreover, they are widely used as interaction means for digital musical instruments, where a complex action-perception loop is involved in the user experience. This is why reestablishing a rich vibrotactile feedback is of key importance for improving the quality of the user's interaction. To the knowledge of the authors, this paper presents the first experiments with Generative Adversarial Networks (GANs) to generate time-reversed signals that can be used to create localized vibrotactile feedback over a rigid surface. The generated signals are sent into an experimental setup and a vibration scan is carried out. A localized peak generated with a signal synthesized by the trained GAN model is observed and studied. Later, different metrics are proposed to evaluate the quality of the generated samples and the obtained localized peak. Finally, a preliminary evaluation of the feasibility of this approach to generate localized vibrations in the range of 200 - 300 Hz for touch-screen applications is discussed.

**Index Terms**—Deep learning, piezoelectric transducer, time-reversal, haptics.

## I. INTRODUCTION

It is of common knowledge that the use of touch-screens for Human-Computer Interaction (HCI) is now standard. Nevertheless, most of the existing devices rely on simplified vibrational, auditive, or visual feedback providing poor feedback to the user which decreases the quality and efficiency of the interaction. It has been demonstrated that the use of rich vibrotactile feedback can increase the quality of multi-touch or multi-user interactions with tactile screens [1].

Digital Musical Instruments (DMIs) are becoming increasingly popular thanks to their large amount of possibilities enabling musicians to increase their expressiveness and encourage creativity. DMIs are generally operated by touch and often use touchscreens to track the position of the finger. Nonetheless, such devices are unable to convey a rich kinesthetic experience. Seeing that, it is important to recover the complex action-perception loop that occurs in traditional acoustic instruments [2], by including a rich and multi-touch vibrotactile feedback on the DMIs.

Several strategies have been developed to achieve localized vibrational feedback over a rigid surface. One can use actuators bonded to the surface and obtain localized vibrations within the area of the actuator [3]. This approach requires a considerable amount of actuators to operate over the whole surface and is affected by the effects of wave propagation

and reverberation. In [4], Pantera et al. use a sparse array of actuators and the inverse filter technique to actively cancel the wave propagation. They obtain localized vibrations in the near field of the actuators reducing the number of actuators that are required. In general, these approaches have led to good results but still require a large amount of actuators that need to be controlled independently. Also, these approaches may limit the possibility of combining transparent touch surfaces with screens for more immersive interaction.

Another method is to exploit the wave propagation phenomenon and control the vibration field over the surface to operate in the far-field of the transducers. Modal synthesis (i.e. modal superposition) has been proposed to create localized peaks [5] [6]. However, there are several limitations on the spatial resolution and contrast ratio (i.e. amplitude of the main peak vs secondary peaks). There is also the time-reversal method which is used to create elastic wave-fronts and obtain localized vibrations. In [7], C. Hudin et al. pre-calibrate the impulse-response between the actuators and several positions on the surface and they are able to increase the amplitude of the peak and improve the contrast ratio by augmenting the number of actuators. In [8], Liu et al. propose a mathematical approach to model the system and obtain the time-reversed impact signals that can create a localized peak while canceling the main secondary peaks, hence, improving the contrast ratio.

To continue improving the contrast ratio and to reduce the number of actuators that are required, it is interesting to study alternative solutions to store and optimize the time-reversed signals that are used to create a localized vibration over a rigid surface. Generative Adversarial Networks (GANs) were first presented by Ian Goodfellow et al. [9] as a strategy to estimate a generative model that captures in a lower-dimensional space the main features of a dataset. As a result, it can generate similar or even new data points. Different domains have benefited from this framework: Image domain [10], Audio domain [11] [12], Time-series data domain [13], more details are presented in section II. Recently there has been certain interest in the applications of GANs for vibrotactile feedback, specifically on the real-time fine-tuning of vibrotactile signals for texture rendering [14] [15].

This paper aims to study the capacity of GANs to capture the distribution of a data-set of time-reversed impacts in a gaussian-like latent space. Once the model is trained, one can randomly draw signals to create localized vibrations, at a desired rate, in the close vicinity of the target point.

\*Project funded by the Swiss National Science Foundation (SNSF # 178972).

In essence, the GANs are trained to synthesize the voltage signals that drive a piezoelectric actuator, bonded to an aluminum beam, to obtain localized vibrations. Later, these signals are sent to an experimental setup to evaluate the quality of the localized peak.

The article is organized as follows. Section II presents an overview of GANs and the motivation to use them for haptic feedback. Then, section III presents the dataset that was used and how the model was trained. Later, section IV contains a collection of the generated signals that are compared to acquired impact signals. It also presents an experimental evaluation of a localized peak that was obtained using a signal generated by the GAN. Finally, section V presents a preliminary evaluation of the feasibility of this approach to generate localized vibrations in the proximity of 250 Hz.

## II. GENERATIVE ADVERSARIAL NETWORKS AND THE IMPLEMENTED MODELS

### A. Generative Adversarial Networks (GANs)

The GAN framework is an approach to training deep generative models. It aims to simultaneously train two models, commonly two multilayer perceptrons, which interact in an adversarial manner [9]. The first model is defined as the generator  $G$ , it aims to capture the distribution of a real dataset  $p_{data}$  (i.e. learning how to up-sample from a lower-dimensional vector drawn from a Gaussian noise distribution  $z \sim p_z$ , into a realistic data sample). The second model is called the discriminator  $D$ , its objective is to estimate the probability that the generated sample  $x$  comes from the real data distribution  $p_{data}$  and not from  $G$  (i.e. classifying the generated sample as real or fake).

Both models are trained simultaneously, in a two-player minimax game, where the parameters of  $G$  are optimized to minimize the value function  $V(D, G)$ , while the parameters of  $D$  are optimized to maximize it:

$$V(D, G) = \mathbb{E}_{x \sim p_{data}} [\log D(x)] + \mathbb{E}_{z \sim p_z} [\log (1 - D(G(z)))] \quad (1)$$

After several iterations, both  $G$  and  $D$  get better at their task and the generator is able to synthesize data samples that become indistinguishable to samples drawn from  $p_{data}$  (i.e.  $x \sim p_g$  very similar to  $x \sim p_{data}$ ). Furthermore, since this approach assumes that  $G$  can model  $p_{data}$  by upsampling from a continuous latent space  $p_z$ , it is possible to interpolate between data points and continuously draw samples from the model.

It means that GANs can be trained in an unsupervised setting where new data can be generated by inputting a latent vector  $z$  to the trained model  $G(z)$ . The general approach to train the GAN is illustrated in Fig. 2a.

### B. GANs for Time-domain Signals

In the last seven years, the use of GANs is becoming popular, in particular for image processing applications where

high resolution and high quality have been achieved. On the contrary, their use for the raw signal domain is just starting. In 2019, Donahue et al. pioneered in this domain [11]. They proposed some adjustments to the DCGAN model [17] to capture the long-term and short-term relations present in audio signals, where the main changes occur along the temporal axis. Several follow-up publications have presented alternative approaches using state-of-the-art architectures and training algorithms that further improve the generation quality for raw audio. For instance, Dieleman et al. [18] use the Progressive Growing Wasserstein GAN (PGAN) and propose an alternative representation of the data that uses the instantaneous frequency to capture the phase of signals, leading to excellent results for highly harmonic signals (e.g. speech and musical instrument sounds). Nistal et al. [12] [19] use the same PGAN architecture but they find that for impact like signals (drum beats) where the phase is extremely chaotic, additional representations such as the waveform and FFT complex representation yield good quality results.

In [11], Donahue et al. propose two approaches to capture the distribution of raw audio data in an unconditioned fashion. The first approach is called SpecGAN, and exploits the DCGAN capabilities for image generation. In a pre-processing step, the raw-audio signals are represented as an image, by transforming the time-domain signal into an amplitude spectrogram using the Short-Time Fourier Transform (STFT). After the generation step, the time-domain signal is retrieved by using the inverse STFT. In this step, the iterative Griffin-Lim algorithm is used to recover the phase information. The second approach is called WaveGAN, in this case, they work directly on the raw-audio representation, by transforming the 2D convolution to a 1D convolution and adding a layer to the DCGAN model. These two models are the base for the experiments presented in this paper.

### C. Motivation for GANs in Haptic Feedback Generation

As mentioned in section I, the time-reversal method and other wave focusing strategies have been used for vibrotactile feedback in rigid surfaces. Furthermore, different academic groups have provided an extensive and successful understanding of the interaction between the actuators and the response of the surface [4] [7] [8]. Nonetheless, the authors of this paper consider there is still room to improve the contrast ratio of the localized peak and to develop alternative strategies to store the time-reversed signals to obtain a localized vibration. One can get inspired by the recent success of GANs on modeling RAW-Audio signals, the diversity of the generated signals, and the similarity in the nature of a time-reversed impact signal with a drum-beat audio signal (i.e. Drum sound effects), more details are given in section III. Thus, one can justify the need to explore the ability of GANs to model the distribution of a dataset containing time-reversed impact signals and/or impulse responses, and evaluate the viability of real-time signal generation to obtain localized vibrations over a rigid surface.

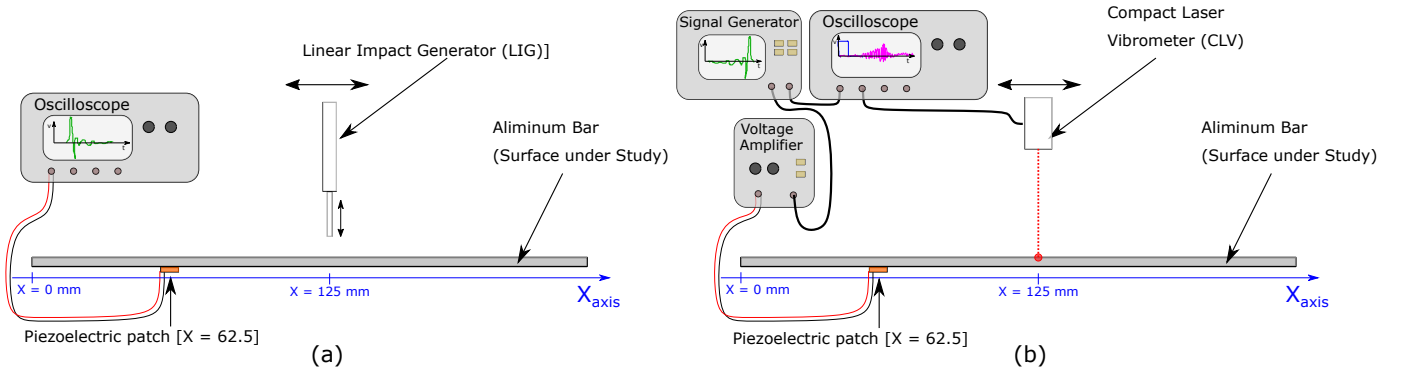


Fig. 1. General approach - a) dataset acquisition mode and b) peak generation and vibration scanning mode.

### III. DATASET AND MODEL TRAINING

Before exploring the dataset and the training of the models, it is important to highlight the similarity between time-reversed impact signals which have been used to localize peaks over a rigid surface [7] [8], and percussive instrument recordings which have been successfully modeled by GANs [11] [19]. The nature behind both types of signals is similar. In both cases impulsive stimuli are applied to a solid medium, initiating a wave propagation that will stimulate the object. From the acquisition point of view, after the stimulus is applied either the stress waves or pressure waves are recorded.

#### A. Time-reversed Impacts Dataset (TrIDS)

An impact dataset was obtained using an improved version of the Linear Impact Generator (LIG) presented in [20]. A pneumatic piston, actuated by a solenoid valve, is mounted on top of a 3-axis CNC table that is controlled by a computer. This system is used to automatically generate, repeatable, mechanical impacts in known positions of an aluminum beam (250 mm x 16 mm x 2mm). This beam has a piezoelectric transducer (Steminc SMPL7W8T02412WL) bond to the surface to acquire the vibrations, as shown in Fig. 1.a.

A total of 5384 impacts were recorded with a sampling rate ( $f_s$ ) of 250 kHz. A detailed description of the dataset acquisition process can be found in section II-B in [21]. Each signal was cropped to a size of 16384 samples and time-reversed (i.e. flip along the time axis). The selected size is defined to keep the original dimension and architecture of the WaveGAN model [11]. For reference, an example of a cropped and time-reversed impact signal is presented in Fig. 3.

For the sake of repeatability and to keep direct compatibility with the original WaveGAN implementation, each sample of the TrIDS is stored in an audio format file [.wav], with a sampling rate ( $f_s$ ) of 250 kHz.

#### B. Discussion on the SpecGAN Model

After several experiments with the SpecGAN model, it can be found that it generates amplitude spectrograms that appear to be of the same nature as an impact signal coming from the original dataset. Nonetheless, the time-domain signal differs both in waveform shape and frequency content.

An explanation for this can be found on the use of the Griffin-Lin iterative algorithm to retrieve the chaotic phase information of the signal. This post-processing method does not result in a reasonable waveform reconstruction to obtain a localized peak. Thus, the SpecGAN approach won't be studied further on this paper and the experiments are carried-out with the WaveGAN model.

#### C. Training of the WaveGAN Model

For the WaveGAN model, the original Tensorflow implementation is used [11]. The data is directly fed from the .wav dataset folder and the signals are loaded with a sample rate of 250000. The hyper-parameters that presented the best results for drum-beat audio representation in [11] were used. To name the most relevant, the batch size is 64 samples, the latent vector dimension is kept to 100, and the phase shuffle parameter is set to 2. The model is trained for 250k iterations (which took around 4.5 days on a Single-NVIDIA 2080Ti GPU system). The model output signals with the same waveform shape and frequency content compared to the real dataset already after 100k iterations (1.5 days).

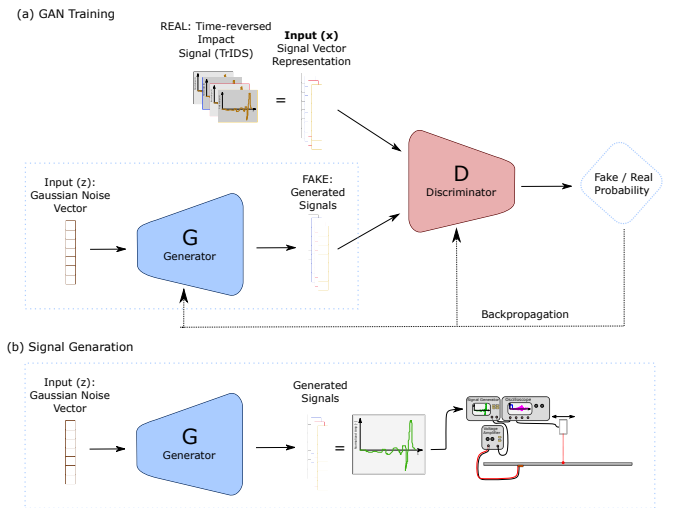


Fig. 2. General approach for training the GAN and representation of the signal generation step. Top (a) GAN Training. Bottom (b) Signal generation and peak generation on the experimental setup.

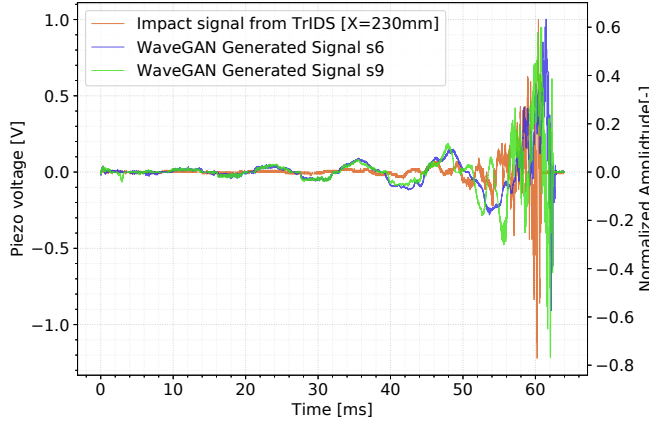


Fig. 3. Signal from the TrIDS for an impact created at position  $X = 230\text{mm}$  and two, randomly picked, time-reversed signals that were generated with the WaveGAN model after it was trained on the TrIDS.

#### D. Frequency Content of a Time-reversed Impact Signal

To better understand the nature of a time-reversed impact one can carry out a frequency analysis of the signal. Fig. 4 presents the magnitude of the FFT of an impact signal coming from the TrIDS. It is possible to observe two main regions with important frequency content. Using the modal analysis module of the ANSYS simulation software, a Finite Element Analysis is carried out to identify the source of these frequency components. It is possible to relate the first range of frequencies (i.e. from 100 Hz to 30 kHz) with the natural frequencies (or eigenmodes) of the mechanical system (i.e. the aluminum bar and the piezoelectric actuator). Then, an impedance analyzer (Agilent 4294A) is used to scan the impedance of the system from the electrical point of view. It was found that the frequencies around 42 kHz match the resonance of the electromechanical system (i.e. the point of lower impedance for the coupled piezoelectric actuator and aluminum beam). This quick analysis helps to form the domain knowledge that can inform the potential metrics to evaluate the performance of the generated signals.

### IV. SIGNAL GENERATION AND EXPERIMENTAL EVALUATION

#### A. Signal Generation

After the model is trained, one or  $n$  samples of time-reversed signals can be synthesized by feeding an array of  $n$  latent vectors  $z$  drawn from the "continuous uniform distribution" (i.e. the same distribution that was used during training). In this case the `numpy.random.rand()` function was used. Fig. 2b displays the process. Also, Fig. 3 presents two signals that are randomly selected from an array of 100 generated signals and compared to a signal from the TrIDS.

#### B. Experimental Setup to Measure the Vibrations Created by the Generated Signals

The LIG setup was modified (i.e. software changes) to acquire the vibrations and study the wave propagation on the

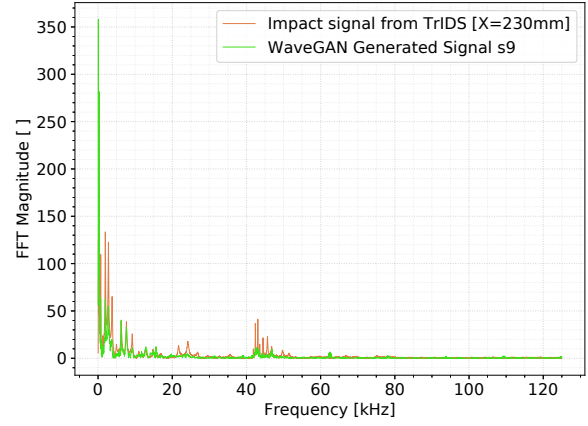


Fig. 4. Example of the frequency domain signal transformation, obtained from a single acquisition, using the Fast Fourier Transform (FFT). This transformation was obtained from the TrIDS signal and signal S9 presented in Fig. 3.

surface of the aluminum bar, after a signal generated with the GAN model is sent as a voltage input to the piezoelectric transducer. The pneumatic actuator, that was used to induce the impacts, is replaced with a Compact Laser Vibrometer (Polytec CLV 100). Then a signal generator (TG5012A) is coupled with a voltage broadband amplifier (TOE7607) to reproduce the generated signal and feed it as an input voltage to the piezoelectric transducer. Since the CLV can only record the displacement in one position at a time, the acquisition is repeated in several positions over the surface of the aluminum bar and the data is superposed. This procedure is illustrated in Fig. 1.b. The acquisition process is as follows:

- The generated signal is transferred to the signal generator and the sampling rate is set.
- A scanning area is defined (In this case the center-line of the aluminum bar).
- The laser spot of the CLV is moved to the first coordinate, using the XYZ table.
- The signal is sent to the piezoelectric actuator, in parallel a trigger signal is sent to the oscilloscope to start the acquisition of the vertical displacement in the surface of the aluminum bar.
- After a short pause to dissipate flexural waves, the laser spot is moved to the next position and the previous step is repeated.

When the acquisition is finished, the signals can be superposed and explored in the time dimension to get an idea of the maximal displacements (i.e. the main peak) and study the wave propagation. The final result is referred to as the vibration scan. An example is presented in figure 5.

The experimental setup was used to obtain a vibration scan of the aluminum bar. In this case, the signal "WaveGAN Generated Signal s9" (that was synthesized by the trained GAN model and presented in Fig. 3) is sent as an input to the system. In Fig. 5 one can observe a localized peak (at position  $X = 230\text{ mm}$ ) right after the generated signal has been reproduced ( $T_{peak} = 62.628\text{ ms}$ ).

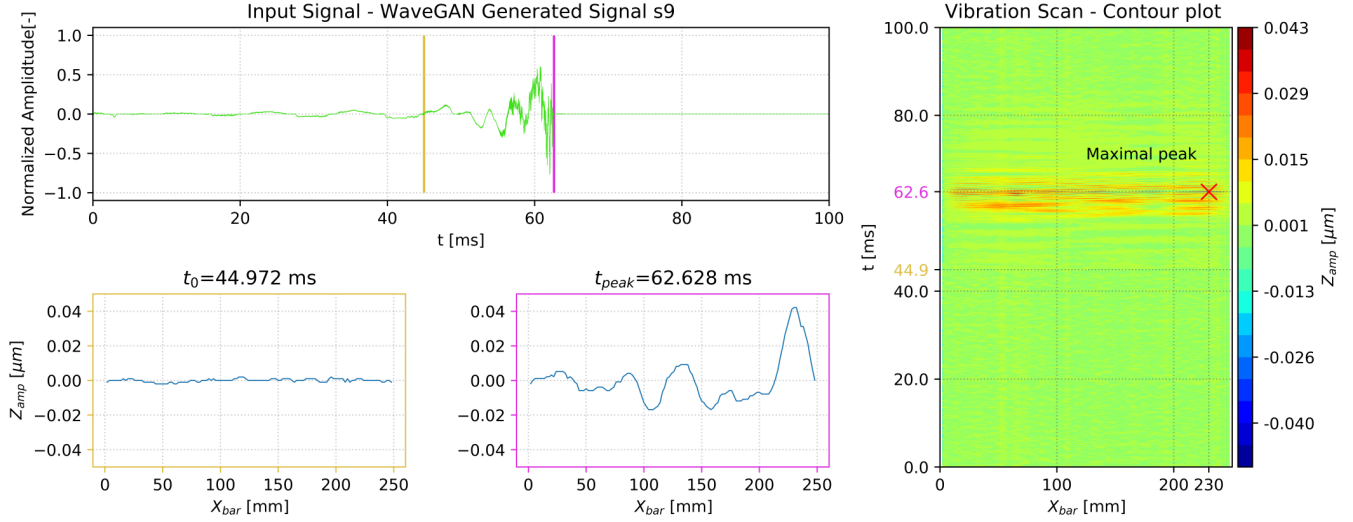


Fig. 5. Visualization of the displacement in the center-line of the aluminum bar at two different instants of the vibration scan. This scan was carried out after sending signal S9 presented in Fig. 3 to the experimental setup. The Upper-Left plot shows the input signal, colored bars indicate each instant of time. The plot on the Right shows the vibration scan contour visualisation (i.e. top view of the displacement at every position of the middle-line of the bar over time). The Lower-Left plots present the displacements occurring in the aluminum bar at a given moment.  $T_{peak}$  is the moment when the maximal displacement appears in position  $X_{peak} = 230 \text{ mm}$ .

### C. Generated Samples Evaluation

In the deep learning community, the quantitative and qualitative metrics that are used to evaluate the quality of the data generated using GANs can still be considered as a work in progress. In terms of qualitative metrics, the most common approach is to rely on expert reviewers (i.e. human evaluators that are familiar with the data that is being modeled). On the other hand, several quantitative metrics have been proposed and compared to human perception. Some involve statistical methods to measure the distance between the generated distribution and the real distribution (e.g. 2-Wasserstein or Fréchet distance). Another metric, known as the "inception score" [23], evaluates the accuracy and diversity of the generated data by penalizing models that generate samples that are not easily classified into a set of known categories as well as models whose samples belong to only a few of the known categories.

Nonetheless, it is important to adjust these metrics for the case of time-reversed impact signals since there is no human expertise on the evaluation of such signals. This is why, this publication proposes alternative low-level feature evaluation metrics, based on the specific domain knowledge and information acquired with the experimental setup. The chosen features are:

- The Location of the main peak after a vibration scan.
- The Contrast ratio (i.e. signal to noise ratio) of the peak after a vibration scan.
- The Frequency content related to the natural frequencies of the bar.

To obtain the location of the maximal peak, the data from the vibration scan, described in section IV-B, is organised as a 3D matrix  $Z_{t, X_{bar}, Z_{amp}}$  where time  $t$ , position  $X$  and vertical displacement  $Z_{amp}$  are the main axes, as shown in the contour

plot in Fig. 5. Then, by projecting the maximal displacement across the  $t$  and  $X_{bar}$  axes, it is possible to find the position  $X_{peak}$  and instant of time  $t_{peak}$  when the maximal peak occurs, an example is presented in figure 5. The contrast ratio  $C_r$ , is defined as the ratio of the the maximum displacement  $Z_{peak}$  over the Root Mean Square (RMS) displacement on the surface at instant  $t_{peak}$ :

$$C_r(t = t_{peak}) = \frac{Z_{peak}}{\sqrt{\frac{1}{n} \sum_{i=1}^n (Z_{amp_1}^2 + \dots + Z_{amp_n}^2)}} \quad (2)$$

For the Vibration scan presented in Fig. 5 the metrics result as follows:  $X_{peak} = 230 \text{ mm}$ ,  $t_{peak} = 62.628 \text{ ms}$ ,  $Z_{peak} = 0.0427 \mu\text{m}$  and  $C_r = 3.87$ . These results are comparable to the peak obtained when the equivalent impact signal from the TrIDS is sent into the system ( $X_{peak} = 230 \text{ mm}$ ,  $t_{peak} = 61.524 \text{ ms}$ ,  $Z_{peak} = 0.0521 \mu\text{m}$  and  $C_r = 3.92$ ). This confirms that the WaveGAN model is able to capture the distribution of the TrIDS and that the generated signals can be used to obtain a localized peak.

### V. REAL-TIME GENERATION AND LOCALIZED VIBRATION FEASIBILITY

The ability of GANs to model and generate time-reversed impact signals has been validated, as well as the presence of a localized peak when the system is fed with the generated signals. It is now imperative to evaluate the feasibility of real-time signal generation and focusing, as well as the possibility to obtain a localized vibration within the range of the human detection threshold [200 - 300 Hz] [24]. To obtain a 200 Hz localized vibration, the signal generation and reproduction should be carried out in less than 5 ms.



Once the GAN model is trained, it is possible to generate a single signal in 3.94 ms. The experimental setup described in section IV-B, was used to measure the reproduction-time to transfer and play-back the signal which took approximately 2 ms.

This leads to a total time of 5.94 ms which is slightly larger than the desired 5ms. Nevertheless, the current evaluation setup is not yet optimized and we are confident that significant improvement can be done in future work. For instance, the generation times can be further reduced by optimizing  $G$  (i.e. reducing the size and number of parameters of the GAN model) and by simplifying the signals to be generated and reproduced (e.g. decrease the length of the signal or generate a 1-bit quantized version as in [7]). Furthermore, the signal reproduction can be optimized by using signal generation hardware that is directly incorporated into the system where the generation is taking place.

## VI. CONCLUSIONS

This paper explores the potential of GANs to capture the distribution of time-reversed impact signals that can be used to obtain localized peaks over a rigid surface. The training and generation process are described, as well as the dataset that is used. This study presents a localized peak created on an aluminum beam after a signal synthesized by the GAN is sent into the experimental setup. As expected, the peak occurs at the desired point. Based on the haptics domain knowledge, different metrics to evaluate the generated signals are presented. These metrics are used to compare the localized peak obtained with a GAN synthesized signal with the peak obtained when a signal from the reference TrIDS is sent into the experimental setup, resulting in a comparable localized peak. Finally, this paper evaluates the feasibility to use the trained generator to synthesize in real-time, signals that can be sent to a piezoceramic transducer to obtain a localized vibration within the human-finger vibrotactile threshold range.

## VII. OUTLOOK AND FUTURE WORK

The authors of this work will continue improving the generation and reproduction process to reach the human-finger vibrotactile threshold range. Then, GANs and Deep Learning in general will be further studied to improve the contrast ratio and number of actuator present in state-of-the-art technics.

## ACKNOWLEDGMENT

The Authors of this paper would like to thank Tatjana Chavdarova, Javier Nistal, Chris Donahue, and Sander Dieleman for the fruitful discussions around their models for image/raw-audio generation using GANs and the potential application on surface haptics.

## REFERENCES

- [1] M. S. Prewett, L. R. Elliott, A. G. Walvoord, and M. D. Coovet, "A Meta-Analysis of Vibrotactile and Visual Information Displays for Improving Task Performance," *IEEE Transactions on Systems, Man, and Cybernetics, Part C (Applications and Reviews)*, vol. 42, no. 1, pp. 123–132, Jan. 2012.
- [2] S. Papetti and C. Saitis, Eds., *Musical Haptics*. Springer International Publishing, 2018.
- [3] S. Papetti, S. Schiesser, and M. Fröhlich, "Multi-Point Vibrotactile Feedback for an Expressive Musical Interface," in *Proceedings of the International Conference on New Interfaces for Musical Expression*, Baton Rouge, Louisiana, USA, 2015, pp. 235–240.
- [4] L. Pantera and C. Hudin, "Multitouch Vibrotactile Feedback on a Tactile Screen by the Inverse Filter Technique: Vibration Amplitude and Spatial Resolution," *IEEE Transactions on Haptics*, vol. 13, no. 3, pp. 493–503, Jul. 2020.
- [5] E. Enferad, C. Giraud-Audine, F. Giraud, M. Amberg, and B. L. Semail, "Generating controlled localized stimulations on haptic displays by modal superimposition," *Journal of Sound and Vibration*, vol. 449, pp. 196–213, Jun. 2019.
- [6] D. Shi, "Modelling of Mechanical Interaction in Piezoelectric Actuated Resonant System," *École Polytechnique Fédérale de Lausanne*, Lausanne, Switzerland, 2016.
- [7] C. Hudin, J. Lozada, and V. Hayward, "Localized Tactile Feedback on a Transparent Surface through Time-Reversal Wave Focusing," *IEEE Transactions on Haptics*, vol. 8, no. 2, pp. 188–198, Apr. 2015.
- [8] X. Liu, "Acoustic emission source detection and wave generation on a working plate using piezoelectric actuators," *École Polytechnique Fédérale de Lausanne*, Lausanne, Switzerland, 2017.
- [9] I. J. Goodfellow et al., "Generative Adversarial Networks," *arXiv:1406.2661 [cs, stat]*, Jun. 2014.
- [10] A. Brock, J. Donahue, and K. Simonyan, "Large Scale GAN Training for High Fidelity Natural Image Synthesis," *arXiv:1809.11096 [cs, stat]*, Feb. 2019.
- [11] C. Donahue, J. McAuley, and M. Puckette, "Adversarial Audio Synthesis," *arXiv:1802.04208 [cs]*, Feb. 2019.
- [12] J. Nistal, S. Lattner, and G. Richard, "Comparing Representations for Audio Synthesis Using Generative Adversarial Networks," *arXiv:2006.09266 [cs, eess]*, Jun. 2020.
- [13] J. Yoon, D. Jarrett, and M. van der Schaar, "Time-series Generative Adversarial Networks," *Advances in Neural Information Processing Systems* 32, pp. 5508–5518, 2019.
- [14] Y. Ujitoko and Y. Ban, "Vibrotactile Signal Generation from Texture Images or Attributes Using Generative Adversarial Network," in *Haptics: Science, Technology, and Applications*, Cham, 2018.
- [15] Y. Ujitoko, Y. Ban, and K. Hirota, "GAN-Based Fine-Tuning of Vibrotactile Signals to Render Material Surfaces," *IEEE Access*, vol. 8, pp. 16656–16661, 2020.
- [16] M. Mirza and S. Osindero, "Conditional Generative Adversarial Nets," *arXiv:1411.1784*, 2014.
- [17] A. Radford, L. Metz, and S. Chintala, "Unsupervised Representation Learning with Deep Convolutional Generative Adversarial Networks," *arXiv:1511.06434 [cs]*, Jan. 2016.
- [18] J. Engel, K. K. Agrawal, S. Chen, I. Gulrajani, C. Donahue, and A. Roberts, "GANSYNTH: ADVERSARIAL NEURAL AUDIO SYNTHESIS," p. 17, 2019.
- [19] J. Nistal, S. Lattner, and G. Richard, "DrumGAN: Synthesis of Drum Sounds With Timbral Feature Conditioning Using Generative Adversarial Networks," *arXiv:2008.12073 [cs, eess]*, Aug. 2020.
- [20] C. H. Mejia, J. Jayet, P. Germano, A. Thabuis, and Y. Perriard, "Linear Impact Generator for Automated Dataset Acquisition of Elastic Waves in Haptic Surfaces," in *2019 22nd International Conference on Electrical Machines and Systems (ICEMS)*, pp. 1–5, Aug. 2019.
- [21] C. H. Mejia, J. Chavanne, P. Germano, and Y. Perriard, "Effect of the Impact Contact Duration on Machine Learning Models for Impact Position Detection," in *2020 23rd International Conference on Electrical Machines and Systems (ICEMS)*, pp. 2063–2068, Nov. 2020.
- [22] "Train Generative Adversarial Network (GAN) for Sound Synthesis - MATLAB & Simulink." <https://www.mathworks.com/help/audio/ug/train-gan-for-sound-synthesis.html>.
- [23] T. Salimans, I. Goodfellow, W. Zaremba, V. Cheung, A. Radford, and X. Chen, "Improved techniques for training GANs," in *Proceedings of the 30th International Conference on Neural Information Processing Systems*, Red Hook, NY, USA, Dec. 2016, pp. 2234–2242.
- [24] R. T. Verrillo, "Vibrotactile thresholds measured at the finger," *Perception & Psychophysics*, vol. 9, no. 4, pp. 329–330, Jul. 1971.